

Study of Cosmic Charged Particle Events with the PolarquEEEst Experiment

Håkon Fossheim

<https://github.com/fosheimdet/FYS5555/tree/master/Project2>

1 Cosmic Rays

Cosmic rays were first discovered in 1912 by Victor Hess on a daring balloon flight where he measured increasing ionization levels with altitude, thus excluding Earth as the source of this radiation. Later measurements during a solar eclipse ruled out the sun as the only source.

The term "cosmic rays" was coined by Robert Millikan in the 1920s who believed the measured ionization stemmed from gamma rays produced as a by product of hydrogen fusion. We now know that cosmic rays consists primarily of charged particles.

Charged particles with an energy of $\sim 10^6 - 10^{20}$ eV reaching the Earth's atmosphere are generally referred to as primary cosmic rays [4]. Low energy cosmic rays are guided by Earth's magnetic field towards the poles while high energy particles can penetrate the magnetic field at any latitude. This is the reason we see a gradual increase in flux from the equator towards the poles. The solar wind provides a steady flux of mostly low energy particles, which cause a saturation point of the flux at a latitude of about 60° N. Upon impact with the atmosphere, primary cosmic rays produce a cascade of secondary particles, called an air shower. When these *secondary cosmic rays* reach the ground, they cover an area of many square kilometers and consist mainly of muons, but also neutrinos, electrons and gamma rays produced primarily through pion decay.

The Pierre Auger observatory [1] located in Argentina detect secondary particles of energies above 10^{18} eV by use of an array of water-Cherenkov detectors covering an area of 3000 km^2 as well as radio and fluorescence detectors to observe the airshowers in the atmosphere. Another experiment that detects high energy cosmic rays is the IceCube observatory in Antarctica, which utilizes the extremely clear ice at depths between 1450 to 2450m to form a massive detector consisting of photomultiplier tubes that trace leptons produced by the neutrinos.

Particles below 10^{17} eV are thought to be produced through diffusive shock acceleration in supernova remnants in our galaxy, but the origin of the

highest energy particles is still unknown. A proposed mechanism for producing these extremely energetic cosmic rays is through reacceleration of lower energy cosmic rays in active galactic nuclei (AGN) [2]. These so-called HZE particles make up about 1% of the nuclei in cosmic rays, with the remaining 87% and 12% consisting of protons and alpha particles respectively. Due to the high energy of these HZE particles, their origin can be traced more easily than lower energy cosmic rays, whose trajectories get bent in interstellar magnetic fields.

2 The POLA detectors

All of the POLA detectors are scintillation detectors. When ionizing radiation hits the scintillator plates of one of the detector, it excites atoms in the scintillation material which proceeds to emit light via luminescence. These photons hit a photocathode, converting the photons to "primary photo electrons" through the photoelectric effect. This signal is far too weak to be measured, and so the signal gets strengthened by going through a silicon photomultiplier (SiPM). The SiPM consists of an array of dynodes at increasing voltages. This creates an electric field between each dynode, accelerating the electrons emitted by the previous dynode in order to produce more electrons after they strike the next dynode. This process repeats itself until there are enough electrons to create a measurable signal. Each POLA detector consists of two planes of four $20 \times 30 \times 1 \text{ cm}^3$ tiles 11cm apart. Each tile is connected to two SiMPs. The trigger condition is set by the coincidence of two signals from a pair of SiMPS of a tile and any other SiMP from the other plane in a time window of 10 ns.

3 Environmental Conditions

The POLA-01 detector was onboard the sailboat Nanuq, which took measurements in a latitude range between 66° N and 82° N on its journey from Ísafjörur (Iceland) to Longyearbyen starting at 22.Juli 2018 and ending at 5.September 2018. The POLA-02 and POLA-03, situated inside highschools at Nesodden in Norway and Bra in Italy respectively, also took measurements in this time period.

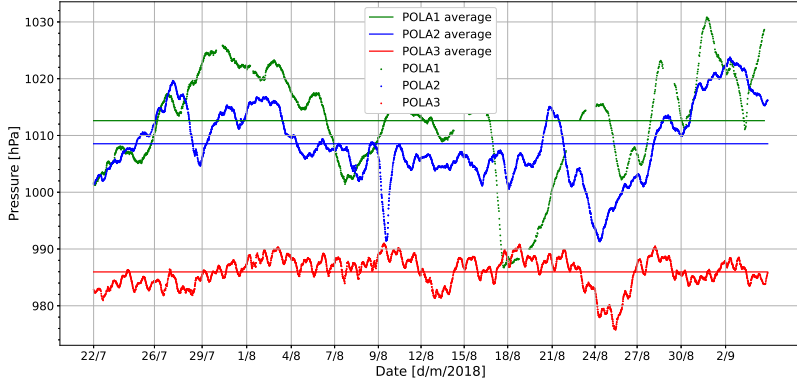


Figure 1: Atmospheric pressure measured by the each of the POLA detectors for the duration of the PolarqEEEst expedition (July 22 - September 5, 2018)

Figure 1 shows the pressure measured by each of the POLA detectors during the expedition. The POLA-03 is situated at an elevation of 310 m, which explains why the pressure reading of this detector is significantly lower than that of POLA-02 (84 m) and POLA-01 (sea level). For the same reason, the POLA-01 pressure readings tend to be higher than both of the detectors, albeit with greater variability.

This is due to its journey, in which it experiences greater weather fluctuations, in particular temperature fluctuations. Comparing figure 2 and 3, we see that the pressure covary with temperature as is to be expected.

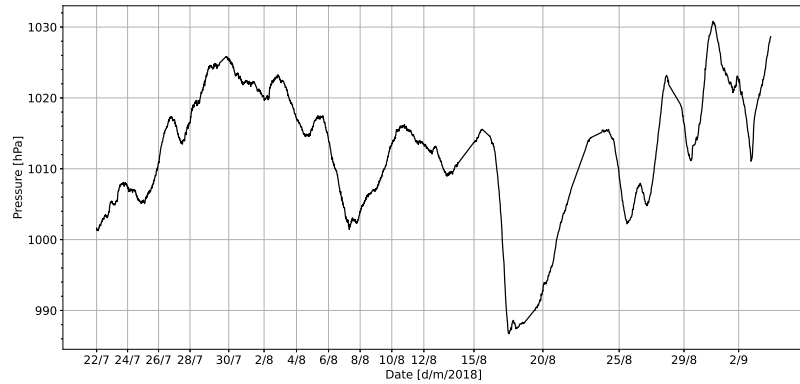


Figure 2: Atmospheric pressure measured by the POLA1 detector for the duration of the PolarqEEEst expedition (July 22 - September 5, 2018)

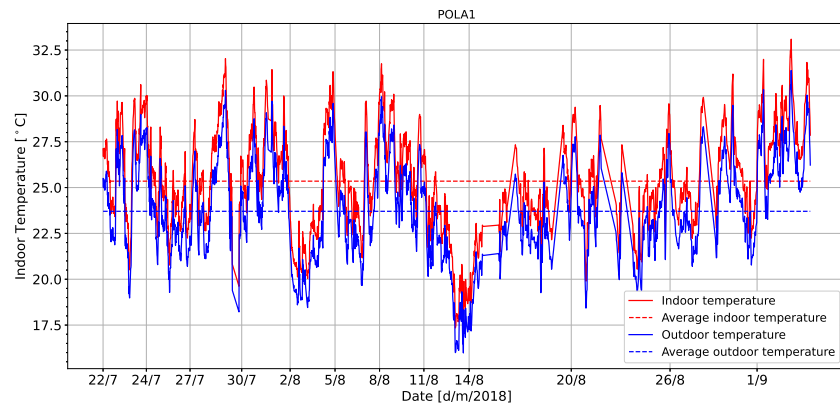


Figure 3: Temperature inside the room of the detector (indoor) and outdoors close to the electronics for the POLA1 detector for duration of the PolarqEEEst expedition (July 22 - September 5, 2018)

Figure 4 and 5 show the indoor and outdoor temperatures of the POLA-02 and POLA-03 detectors respectively.

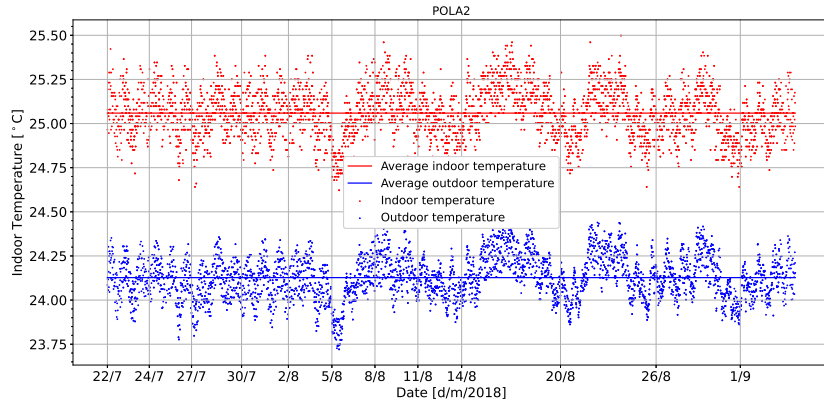


Figure 4: POLA2 indoor vs outdoor temperature

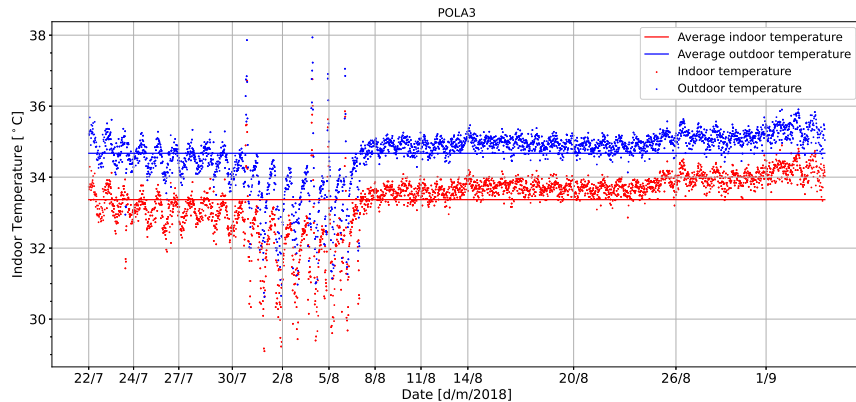


Figure 5: POLA3 indoor vs outdoor temperature

4 Particle Raw Rate

Figure 6 shows the raw rate as a function of time. Due to latitude we see that the POLA-01 and POLA-02 raw rates are higher than that of POLA-03. The raw rates for POLA-01 and POLA-02 are quite similar due to the aforementioned saturation point in latitude. We can however see a slight covariance with latitude for the POLA-01 raw rate.

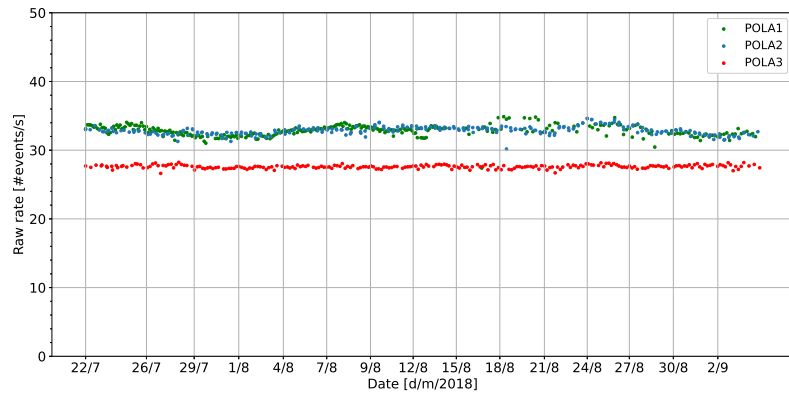


Figure 6: Raw rate measured by each of the detectors for the duration of the PolarqEEEst expedition (July 22 - September 5, 2018)

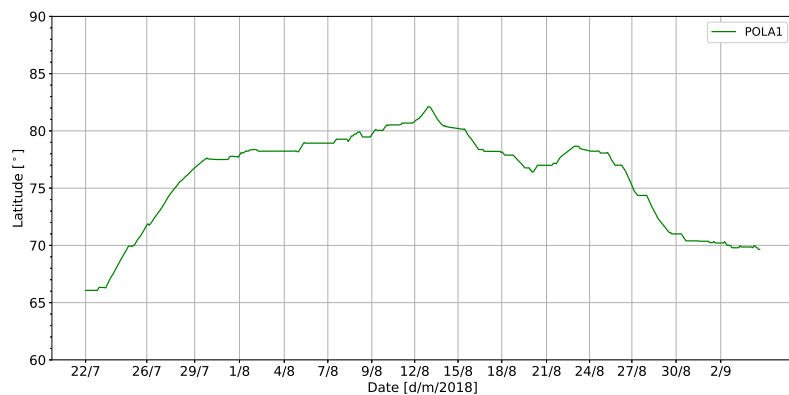


Figure 7: Latitude of the POLA-01 detector throughout its journey.

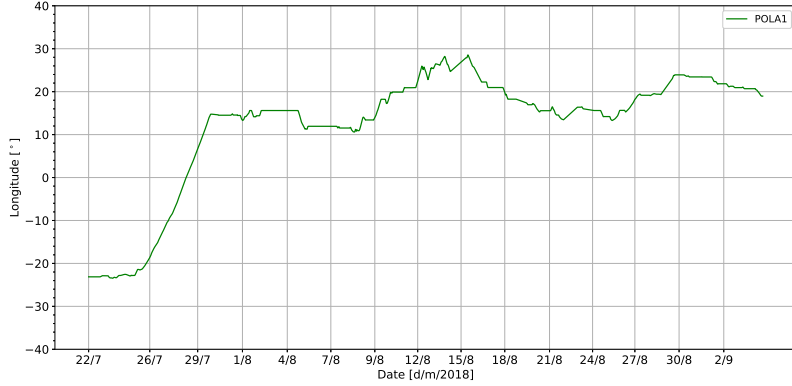


Figure 8: Longitude of the POLA-01 detector throughout its journey.

As the temperature of the atmosphere increases, it expands and causes primary cosmic rays to interact at higher altitudes. In order to account for atmospheric expansion, we would need temperature measurements of different air layers in order to calculate an effective temperature for the atmospheric column above each detector or we could use e.g. the mean altitude of pion creation.

We only have temperature measurements at the detector locations, which will not in and of itself affect the raw rates. Figure 9 indeed shows the raw rate to be rather independent of the local temperature.

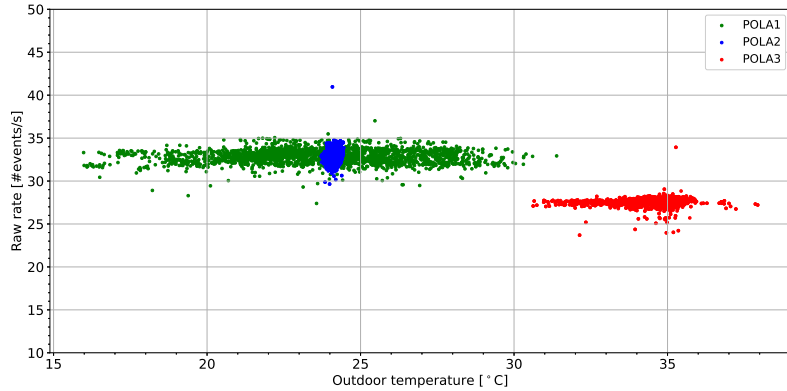


Figure 9: Raw rate vs. outdoor temperature for each of the detectors for the duration of the PolarqEEEst expedition (July 22 - September 5, 2018)

An important variable which affects the raw rate of the detectors is the

barometric pressure. The barometric pressure reflects the atmospheric thickness above the detector, thus yielding a lower rate at higher pressures due to increased energy loss in the secondary cosmic rays. Let N be the raw rate and p be the atmospheric pressure measured by the detector. We then have

$$\frac{dN}{N} = \beta dp \quad (1)$$

Where $\beta < 0$. Equation 1 used the fractional raw rate, as an airshower with higher flux will yield a larger increase in raw rate than that of an airshower with lower flux for the same reduction in pressure. Integrating this equation gives

$$\begin{aligned} \int_{N_{ref}}^N \frac{1}{N'} dN' &= \int_{p_{ref}}^p \beta dp' \\ N &= N_{ref} e^{\beta(p - p_{ref})} \end{aligned} \quad (2)$$

p_{ref} is a reference pressure, estimated from the total average pressure over the complete time period. N_{ref} is the hypothetical raw rate at this pressure, found through linear regression. Note that this choice of reference pressure is arbitrary. Now we may incorporate the variations in the primary cosmic ray flux stemming mainly from solar activity through the variable ν [3]:

$$\begin{aligned} N &= N_{ref}(1 + \nu)e^{\beta(p - p_{ref})} \\ N &= N_{ref}e^{\alpha + \beta(p - p_{ref})} \end{aligned}$$

Where $\alpha = \ln(1 + \nu)$. Determining α requires a reference detector with measurements of the same rigidity during a period of low solar activity, which we lack to my awareness. The variability in primary cosmic flux will therefore be ignored, and the focus will lie on correcting for atmospheric pressure.

Because the pressure variations of each detector is relatively ¹ small, we may make the following approximation

$$N \approx N_{ref}(1 + \beta(p - p_{ref})) \quad (3)$$

¹Relative to p_{ref}

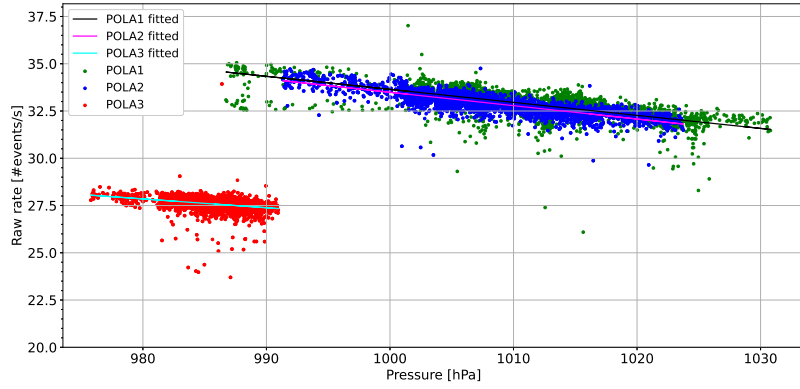


Figure 10: Raw rate vs. pressure for each of the detectors for the duration of the PolarqEEEst expedition (July 22 - September 5, 2018)

Figure 10 shows the raw rate as a function of pressure for the three detectors. By using linear regression, a best fit was found for the data was found in order to determine N_{ref} . According to equation 3, β is then found by dividing the slope by N_{ref} . The results for each of the detectors are shown in the table below.

	POLA-01	POLA-02	POLA-03
p_{ref} [mbar]	1011.85	1008.53	985.87
N_{ref}	32.8296	32.886	27.5751
β	-0.00209806	-0.00214959	-0.00169461

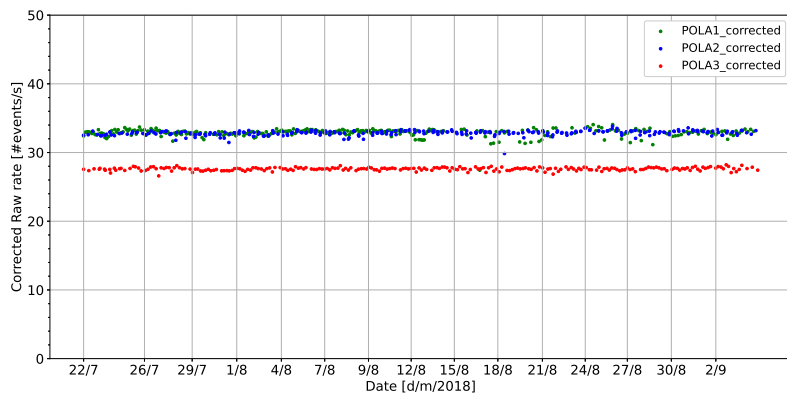


Figure 11: Corrected raw rate vs. pressure

In order to find the raw rate "normalized" to p_{ref} , viz. the corrected raw rate, we must divide the uncorrected raw rate by the barometric correction coefficient is given by

$$\gamma(p) = e^{\beta(p-p_{ref})} \approx (1 + \beta(p - p_{ref})) \quad (4)$$

Figure 11 shows this corrected raw rate plotted against time. Comparing with figure 6, we see that the data has significantly flattened out due to removing the atmospheric pressure dependence.

References

- [1] Stefan Fliescher. "Radio detection of cosmic ray induced air showers at the Pierre Auger Observatory". In: *Nuclear Instruments and Methods in Physics Research Section A: Accelerators, Spectrometers, Detectors and Associated Equipment* 662 (2012). 4th International workshop on Acoustic and Radio EeV Neutrino detection Activities, S124–S129. ISSN: 0168-9002. DOI: <https://doi.org/10.1016/j.nima.2010.11.045>. URL: <http://www.sciencedirect.com/science/article/pii/S0168900210025088>.
- [2] Rostom Mbarek and Damiano Caprioli. "Bottom-up Acceleration of Ultra-high-energy Cosmic Rays in the Jets of Active Galactic Nuclei". In: *The Astrophysical Journal* 886.1 (Nov. 2019), p. 8. DOI: 10.3847/1538-4357/ab4a08. URL: <https://doi.org/10.3847%2F1538-4357%2Fab4a08>.
- [3] P. Paschalis et al. "Online application for the barometric coefficient calculation of the NMDB stations". In: *New Astronomy* 19 (2013), pp. 10–18. ISSN: 1384-1076. DOI: <https://doi.org/10.1016/j.newast.2012.08.003>. URL: <http://www.sciencedirect.com/science/article/pii/S1384107612000759>.
- [4] Omar Tibolla and Roger D. Blandford. "Cosmic Ray Origin – Beyond the Standard Models". In: *Nuclear and Particle Physics Proceedings* 297-299 (2018). Cosmic Ray Origin - Beyond the Standard Models, pp. 1–5. ISSN: 2405-6014. DOI: <https://doi.org/10.1016/j.nuclphysbps.2018.07.001>. URL: <http://www.sciencedirect.com/science/article/pii/S2405601418300865>.